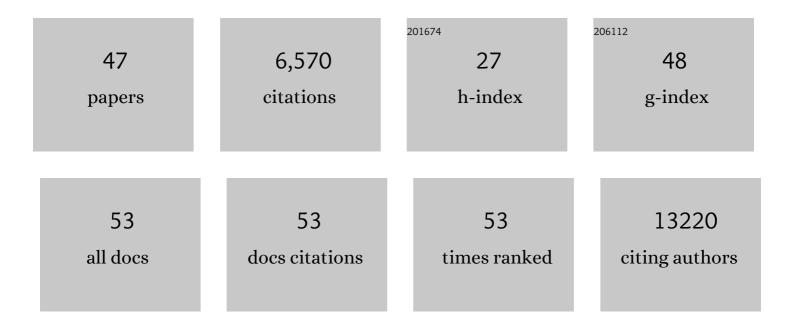
Yuguang Zhao

List of Publications by Year in descending order

Source: https://exaly.com/author-pdf/1876763/publications.pdf Version: 2024-02-01



Унсилыс 7нло

#	Article	IF	CITATIONS
1	Broad and strong memory CD4+ and CD8+ T cells induced by SARS-CoV-2 in UK convalescent individuals following COVID-19. Nature Immunology, 2020, 21, 1336-1345.	14.5	1,066
2	Evidence of escape of SARS-CoV-2 variant B.1.351 from natural and vaccine-induced sera. Cell, 2021, 184, 2348-2361.e6.	28.9	936
3	Reduced neutralization of SARS-CoV-2 B.1.617 by vaccine and convalescent serum. Cell, 2021, 184, 4220-4236.e13.	28.9	630
4	Antibody evasion by the P.1 strain of SARS-CoV-2. Cell, 2021, 184, 2939-2954.e9.	28.9	519
5	Reduced neutralization of SARS-CoV-2 B.1.1.7 variant by convalescent and vaccine sera. Cell, 2021, 184, 2201-2211.e7.	28.9	442
6	Neutralizing nanobodies bind SARS-CoV-2 spike RBD and block interaction with ACE2. Nature Structural and Molecular Biology, 2020, 27, 846-854.	8.2	434
7	The antigenic anatomy of SARS-CoV-2 receptor binding domain. Cell, 2021, 184, 2183-2200.e22.	28.9	331
8	Neutralization of SARS-CoV-2 by Destruction of the Prefusion Spike. Cell Host and Microbe, 2020, 28, 445-454.e6.	11.0	298
9	Structural basis for the neutralization of SARS-CoV-2 by an antibody from a convalescent patient. Nature Structural and Molecular Biology, 2020, 27, 950-958.	8.2	268
10	Toremifene interacts with and destabilizes the Ebola virus glycoprotein. Nature, 2016, 535, 169-172.	27.8	210
11	Critical Role of the Virus-Encoded MicroRNA-155 Ortholog in the Induction of Marek's Disease Lymphomas. PLoS Pathogens, 2011, 7, e1001305.	4.7	157
12	Picornavirus uncoating intermediate captured in atomic detail. Nature Communications, 2013, 4, 1929.	12.8	148
13	Neutralization potency of monoclonal antibodies recognizing dominant and subdominant epitopes on SARS-CoV-2 Spike is impacted by the B.1.1.7 variant. Immunity, 2021, 54, 1276-1289.e6.	14.3	112
14	The crystal structure of human dopamine β-hydroxylase at 2.9 à resolution. Science Advances, 2016, 2, e1500980.	10.3	80
15	Lysosome sorting of \hat{l}^2 -glucocerebrosidase by LIMP-2 is targeted by the mannose 6-phosphate receptor. Nature Communications, 2014, 5, 4321.	12.8	78
16	Unexpected mode of engagement between enterovirus 71 and its receptor SCARB2. Nature Microbiology, 2019, 4, 414-419.	13.3	73
17	Target Identification and Mode of Action of Four Chemically Divergent Drugs against Ebolavirus Infection. Journal of Medicinal Chemistry, 2018, 61, 724-733.	6.4	66
18	Automation of large scale transient protein expression in mammalian cells. Journal of Structural Biology, 2011, 175, 209-215.	2.8	55

YUGUANG ZHAO

#	Article	IF	CITATIONS
19	The antibody response to SARS-CoV-2 Beta underscores the antigenic distance to other variants. Cell Host and Microbe, 2022, 30, 53-68.e12.	11.0	52
20	Structural Insights into the Inhibition of Wnt Signaling by Cancer Antigen 5T4/Wnt-Activated Inhibitory Factor 1. Structure, 2014, 22, 612-620.	3.3	42
21	Crystal Structure of Insulin-Regulated Aminopeptidase with Bound Substrate Analogue Provides Insight on Antigenic Epitope Precursor Recognition and Processing. Journal of Immunology, 2015, 195, 2842-2851.	0.8	41
22	Structure of glycosylated <scp>NPC</scp> 1 luminal domain C reveals insights into <scp>NPC</scp> 2 and Ebola virus interactions. FEBS Letters, 2016, 590, 605-612.	2.8	39
23	Structures of Ebola Virus Glycoprotein Complexes with Tricyclic Antidepressant and Antipsychotic Drugs. Journal of Medicinal Chemistry, 2018, 61, 4938-4945.	6.4	38
24	X-Ray Crystal Structure of the Full Length Human Chitotriosidase (CHIT1) Reveals Features of Its Chitin Binding Domain. PLoS ONE, 2016, 11, e0154190.	2.5	34
25	Structure-Based in Silico Screening Identifies a Potent Ebolavirus Inhibitor from a Traditional Chinese Medicine Library. Journal of Medicinal Chemistry, 2019, 62, 2928-2937.	6.4	34
26	Ligand-Induced Conformational Change of Insulin-Regulated Aminopeptidase: Insights on Catalytic Mechanism and Active Site Plasticity. Journal of Medicinal Chemistry, 2017, 60, 2963-2972.	6.4	33
27	Structure of the Dual-Mode Wnt Regulator Kremen1 and Insight into Ternary Complex Formation with LRP6 and Dickkopf. Structure, 2016, 24, 1599-1605.	3.3	32
28	Hand-foot-and-mouth disease virus receptor KREMEN1 binds the canyon of Coxsackie Virus A10. Nature Communications, 2020, 11, 38.	12.8	28
29	New insights into the enzymatic mechanism of human chitotriosidase (CHIT1) catalytic domain by atomic resolution X-ray diffraction and hybrid QM/MM. Acta Crystallographica Section D: Biological Crystallography, 2015, 71, 1455-1470.	2.5	23
30	Discovery of 2-phenoxyacetamides as inhibitors of the Wnt-depalmitoleating enzyme NOTUM from an X-ray fragment screen. MedChemComm, 2019, 10, 1361-1369.	3.4	22
31	Structural characterization of melatonin as an inhibitor of the Wnt deacylase Notum. Journal of Pineal Research, 2020, 68, e12630.	7.4	21
32	Antiepileptic Drug Carbamazepine Binds to a Novel Pocket on the Wnt Receptor Frizzled-8. Journal of Medicinal Chemistry, 2020, 63, 3252-3260.	6.4	20
33	Stereotyped antibody responses target posttranslationally modified gluten in celiac disease. JCI Insight, 2017, 2, .	5.0	20
34	Notum deacylates octanoylated ghrelin. Molecular Metabolism, 2021, 49, 101201.	6.5	17
35	Structure of the Wnt signaling enhancer <scp>LYPD</scp> 6 and its interactions with the Wnt coreceptor <scp>LRP</scp> 6. FEBS Letters, 2018, 592, 3152-3162.	2.8	13
36	Scaffold-hopping identifies furano[2,3-d]pyrimidine amides as potent Notum inhibitors. Bioorganic and Medicinal Chemistry Letters, 2020, 30, 126751.	2.2	13

Yuguang Zhao

#	Article	IF	CITATIONS
37	5-Phenyl-1,3,4-oxadiazol-2(3 <i>H</i>)-ones Are Potent Inhibitors of Notum Carboxylesterase Activity Identified by the Optimization of a Crystallographic Fragment Screening Hit. Journal of Medicinal Chemistry, 2020, 63, 12942-12956.	6.4	13
38	Small-molecule inhibitors of carboxylesterase Notum. Future Medicinal Chemistry, 2021, 13, 1001-1015.	2.3	13
39	Poly(A) Binding Protein 1 Enhances Cap-Independent Translation Initiation of Neurovirulence Factor from Avian Herpesvirus. PLoS ONE, 2014, 9, e114466.	2.5	12
40	Screening of a Custom-Designed Acid Fragment Library Identifies 1-Phenylpyrroles and 1-Phenylpyrrolidines as Inhibitors of Notum Carboxylesterase Activity. Journal of Medicinal Chemistry, 2020, 63, 9464-9483.	6.4	12
41	Caffeine inhibits Notum activity by binding at the catalytic pocket. Communications Biology, 2020, 3, 555.	4.4	11
42	Design of a Potent, Selective, and Brain-Penetrant Inhibitor of Wnt-Deactivating Enzyme Notum by Optimization of a Crystallographic Fragment Hit. Journal of Medicinal Chemistry, 2022, 65, 7212-7230.	6.4	9
43	Structural Insights into Notum Covalent Inhibition. Journal of Medicinal Chemistry, 2021, 64, 11354-11363.	6.4	8
44	Virtual Screening Directly Identifies New Fragment-Sized Inhibitors of Carboxylesterase Notum with Nanomolar Activity. Journal of Medicinal Chemistry, 2022, 65, 562-578.	6.4	8
45	Structures and therapeutic potential of anti-RBD human monoclonal antibodies against SARS-CoV-2. Theranostics, 2022, 12, 1-17.	10.0	6
46	Structural Analysis and Development of Notum Fragment Screening Hits. ACS Chemical Neuroscience, 2022, 13, 2060-2077.	3.5	3
47	Reduced Neutralization of SARS-CoV-2 B.1.1.7 Variant from Naturally Acquired and Vaccine Induced	0.4	2